

Efficient Haze Removal by Edge Detection and Colour Attenuation

Asakti Rautkar¹, Pugal Priya Rajasaviour², Dr.D.B.Salunke³

¹*Asst.Prof, P.G. Moze COE, Pune*

²*Dean(Acad), P.G. Moze COE, Pune*

Abstract - Haze removal is a prominent query faced due to varying weather conditions. Here, we try to rectify the issue by edge detection of the image and color attenuation on the image. Knowing the depth map of the image and using it to estimate the transmission and restoring the scene radiance via the atmospheric model, the haze value can be reduced. The proposed method requires only a few general assumptions and can restore a high-quality haze-free image with faithful colour and fine image details.

Keywords: Processing Depth map, Edge Detection, Dehazing, Image.

I. INTRODUCTION

Images fetch in Bad weather (fog or Haze) lose their contrast and fidelity as light is absorbed and scattered by the turbid medium such as particles and water droplets in the atmosphere during propagation. It also leads to the colours of these objects get faded and become much similar to the fog, the similarity of which depending on the distances of them to the camera. System which works on the image perception often get a false in put due to such images, haze removal methods are of prime importance in image understanding and computer applications such as aerial imagery[1], image classification[2]-[5],image/video retrieval[6]-[8], remote sensing[9]-[11] and video analysis and recognition[12].

The concentration of haze varies from place to place and it is difficult to detect information in a hazy image, hence haze removal is an essential and challenging work. Since a single image hardly contains much information so the traditional techniques such as Histogram detection aren't efficient. In [8] and [2], polarization based methods are used for Dehazing with multiple images which are taken with different degrees of polarization. Narasimhan et al. Propose haze removal approaches with multiple images of the same scene under different weather conditions [1]-[3]. Dehazing can also be done by knowing the depth information [4]-[5].

Hazy images have lesser contrast as compared to hazy free images. Tan [6] proposes a novel hazy removal method by maximizing the local contrast of the image based on Markov Random Field (MRF). This approach produces

over saturated images even though it achieves impressive results.

Fattal [11] proposed to remove the hazy from colour images based on independent component analysis (ICA). His approach is not applicable for gray scale images and consumes time. He et al. [9] discover the dark channel prior (DCP) that, in most of the non- sky patches, at least one colour channel has some pixels whose intensities are very low and closed to zero. Atmospheric scattering model is used to restore the hazy free image by estimating the thickness of haze. Tarel and Hautiere and Tarel et al.[8] replace the time consuming soft matting with standard median filtering, "Median of Median filter", guided joint bilateral filtering and guided image filtering respectively. Meng et al. [9] propose an effective regularization Dehazing method to restore the haze-free image by exploring the inherent boundary constraint; Tang et al. combine four types of haze-relevant features with Random Forest to estimate the transmission.

II. ATMOSPHERIC SCATTERING MODEL

The model is widely used in computer vision and image processing and the model can be expressed as follows:

$$I(x) = J(x)t(x) + A(1 - t(x)), \quad (1)$$
$$t(x) = e^{-\beta d(x)} \quad (2)$$

Where x is the position of the pixel within the image, I is the haze image, J is the scene radiance representing the haze-free image, A is the atmospheric light, t is the medium of transmission, β is the scattering coefficient of the atmosphere and d is the depth of scene. I, J and A are all three dimensional vectors in RGB space. Since I is known, the goal of dehazing is to estimate A and t , then restore J according to equation (1). In a ideal case, the range of $d(x)$ is $[0, +\infty)$, where the objects that appear in the image can be very far from the observer, and we have:

$$I(x)=A, \quad d(x) \rightarrow \infty \quad \square$$

If $d(x)$ is large enough, $t(x)$ tends to be very small according to equation (2), and $I(x)$ equals A approximately. Therefore instead of calculating the

atmospheric light A by equation (3) it can be done by following one, $d_{\text{threshold}}$:

$$I(x) = A, \quad d(x) \leq d_{\text{threshold}}. \quad (4)$$

In most cases, a hazy images taken outdoor has a distant view that is kilometres away from the observer and the pixel belonging to the region with a distant view in the image should have a very large depth, $d_{\text{threshold}}$

III. COLOUR ATTENUATION PRIOR

Upon analysis it was conferred that the brightness and the saturation of pixels in a hazy image vary sharply along with the change of the haze concentration. In a haze-free region, the saturation of the scene is pretty high, the brightness is moderate and the difference between the brightness and the saturation is close to zero. While the saturation of the patch decreases sharply while the colour of the scene fades under the influence of the haze, and the brightness increases at the same time producing the high value of the difference. In a dense-haze region, it is more difficult for us to recognize the inherent colour of the scene, and the difference is even higher. In the haze-free condition, the scene element reflects the energy that is from the illumination source (e.g., direct sunlight, diffuse skylight and light reflected by the ground), and little energy is lost when it reaches the imaging system. The imaging system collects the incoming energy reflected from the scene element and focuses it onto the image plane

In hazy weather, in contrast, the situation becomes more complex. There are two mechanisms (the direct attenuation and the air light) in imaging under hazy weather. The term $J(x)$ (x) in Equation (1) is used for describing the direct attenuation. It reveals the fact that the intensity of the pixels within the image will decrease in a multiplicative manner. So it turns out that the brightness tends to decrease under the influence of the direct attenuation. On the other hand, the white or gray airlight, which is formed by the scattering of the environmental illumination, enhances the brightness and reduces the saturation. It is found out that the effect of the white or gray airlight on the observed values is additive. Thus, caused by the airlight, the brightness is increased while the saturation is decreased. Since the air light plays a more important role in most cases, hazy regions in the image are characterized by high brightness and low saturation.

As the concentration of the haze increases along with the change of the scene depth in general, we have made an assumption that the depth of the scene is positively correlated with the concentration of the haze and we have:

$$d(x) \propto c(x) \propto v(x) - s(x) \quad (5)$$

Where d is the scene depth, c is the concentration of the haze, v is the brightness of the scene and s is the saturation. In the colour model of HSV if α varies between zero and 90 degrees, the higher the value of α will be the tangent of α . This denotes the greater the difference between the component of I in the direction of V and the component of I in the direction of S . As the depth increases, the value of v increases and the saturation s decreases and therefore α increases.

IV. SCENE DEPTH RESTORATION

The linear model definition:

As the difference between the brightness and saturation can approximately represent the concentration of the haze. Thus a linear model can be created as follows:

$$d(x) = \theta_0 + \theta_1 v(x) + \theta_2 s(x) + \mathcal{E}(x), \quad (6)$$

Where x is the position within the image, d is the scene depth, v is the brightness component of the hazy image, s is the saturation component, $\theta_0, \theta_1, \theta_2$ are the unknown linear coefficients, $\mathcal{E}(x)$ is a random variable representing the random error of the model and \mathcal{E} can be regarded as a random image. Gaussian density for \mathcal{E} with zero mean variable σ^2 is used. According to the property of the Gaussian distribution

$$d(x) \sim p(d(x)|x, \theta_0, \theta_1, \theta_2, \sigma^2) = N(\theta_0 + \theta_1 v(x) + \theta_2 s, \sigma^2) \quad (7)$$

The prime importance of the model is that its edge preserving property, the gradient d we can do that by the equation

$$\nabla d = \theta_1 \nabla v + \theta_2 \nabla s + \nabla \mathcal{E} \quad (8)$$

Due to that σ can never be too large in practice the value of $\mathcal{E}(x)$ tends to be very low and close to zero. Both the gradient image $\nabla \mathcal{E}$ and the random image \mathcal{E} are very dark. It turns out that the edge distribution of d is independent of \mathcal{E} given a small σ . In addition, since v and s are actually the two single-channel images (the value channel and the saturation channel of the HSV colour space) into which the hazy image I splits, Equation (10) ensures that d has an edge only if I has an edge.

Sobel Edge Detector

The Sobel operator performs a 2-D spatial gradient measurement on an image and so emphasizes regions of high spatial frequency that correspond to edges. Typically it is used to find the approximate absolute gradient magnitude at each point in an input grayscale image. The

Sobel operator is slower to compute than the Roberts Cross operator, but its larger convolution kernel smooths the input image to a greater extent and so makes the operator less sensitive to noise. The operator also generally produces considerably higher output values for similar edges, compared with the Roberts Cross.

As with the Roberts Cross operator, output values from the operator can easily overflow the maximum allowed pixel value for image types that only support smallish integer pixel values. When this happens the standard practice is to simply set overflowing output pixels to the maximum allowed value. The problem can be avoided by using an image type that supports pixel values with a larger range. Natural edges in images often lead to lines in the output image that are several pixels wide due to the smoothing effect of the Sobel operator. Some thinning may be desirable to counter this. Failing that, some sort of hysteresis ridge tracking could be used as in the Canny operator.

Prewitt edge detector

It is also called as compass edge detector. Compass Edge Detection is an alternative approach to the differential gradient edge detection. The operation usually outputs two images, one estimating the local edge gradient magnitude and one estimating the edge orientation of the input image. When using compass edge detection the image is convolved with a set of convolution kernels, each of which is sensitive to edges in a different orientation. For each pixel the local edge gradient magnitude is estimated with the maximum response of all 8 kernels at this pixel location

Robert Cross edge detector

According to Roberts, an edge detector should have the following properties: the produced edges should be well-defined, the background should contribute as little noise as possible and the intensity of edges should correspond as close as possible to what a human would perceive. With these criteria in mind and based on then prevailing psychophysical theory Roberts proposed the following equations:

$$y_{i,j} = \sqrt{x_{i,j}} \quad (9)$$

$$z_{i,j} = \sqrt{(y_{i,j} - y_{i+1,j+1})^2 + (y_{i+1,j} - y_{i,j+1})^2} \quad (10)$$

where x is the initial intensity value in the image, z is the computed derivative and i,j represent the location in the image. The results of this operation will highlight changes in intensity in a diagonal direction. One of the most

appealing aspects of this operation is its simplicity; the kernel is small and contains only integers. However with the speed of computers today this advantage is negligible and the Roberts cross suffers greatly from sensitivity to noise.

V. EXPERIMENTAL RESULTS

In order to verify the effectiveness of the proposed dehazing method, we test it on various hazy images and compare Meng et al.'s methods. All the algorithms are implemented in the MatlabR2013a environment on a CORE i3-3.3GHz PC with 4GB RAM. The parameters used in the proposed method are initialized as follows: $r = 15$, $\beta = 1.0$, $\theta_0 = 0.121779$, $\theta_1 = 0.959710$, $\theta = -0.780245$ and $s = 0.041337$. For fair comparison, the parameters used in the four popular dehazing methods are set to be optimal.



Fig.5.1 Haze images





Fig.5.2 Depth Maps



Fig.5.3 Haze-free Images

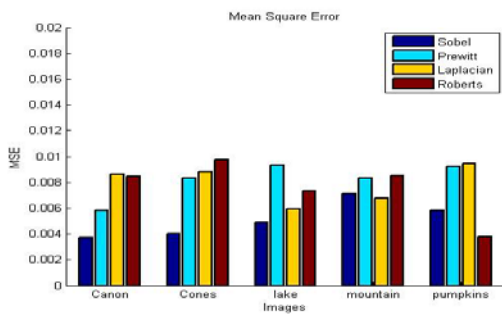


Fig.5.4 MSE of each Images

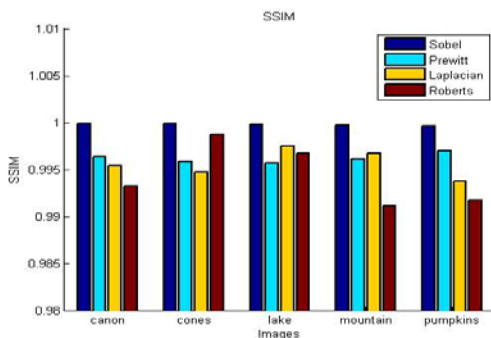


Fig.5.5 SSIM of each Images

REFERENCES

[1] L. Shao, L. Liu, and X. Li, "Feature learning for image classification via multiobjective genetic programming," *IEEE Trans. Neural Netw. Learn. Syst.*, vol. 25, no. 7, pp. 1359–1371, Jul. 2014.

[2] F. Zhu and L. Shao, "Weakly-supervised cross-domain dictionary learning for visual recognition," *Int. J. Comput. Vis.*, vol. 109, os. 1–2, pp. 42–59, Aug. 2014.

[3] Y. Luo, T. Liu, D. Tao, and C. Xu, "Decomposition-based transfer distance metric learning for image classification," *IEEE Trans. Image Process.*, vol. 23, no. 9, pp. 3789–3801, Sep. 2014.

[4] J. Han et al., "Representing and retrieving video shots in human-centric brain imaging space," *IEEE Trans. Image Process.*, vol. 22, no. 7, pp. 2723–2736, Jul. 2013.

[5] K. He, J. Sun, and X. Tang, "Single image haze removal using dark channel prior," *IEEE Trans. Pattern Anal. Mach. Intell.*, vol. 33, no. 12, pp. 2341–2353, Dec. 2011.

[6] Q. Zhu, S. Yang, P. A. Heng, and X. Li, "An adaptive and effective single image dehazing algorithm based on dark channel prior," in *Proc. IEEE Conf. Robot. Biomimetics (ROBIO)*, Dec. 2013, pp. 1796–1800.

[7] Y. Xiang, R. R. Sahay, and M.S.Kankanhalli, "Hazy image enhancement based on the full-saturation assumption," in *Proc. IEEE Conf. Multimedia Expo workshops (ICMEW)*, Jul. 2013, pp. 1–4.

[8] C. O. Ancuti, C. Ancuti, C. Hermans, and P. Bekaert, "A fast semiinverse approach to detect and remove the haze from a single image," in *Proc. Asian Conf. Comput. Vis. (ACCV)*, 2010, pp. 501–514.

[9] G. F. Meng, Y. Wang, J. Duan, S. Xiang, and C. Pan, "Efficient image dehazing with boundary constraint and contextual regularization," in *Proc. IEEE Int. Conf. Comput. Vis. (ICCV)*, Dec. 2013, pp. 617–624.

[10] K. Tang, J. Yang, and J. Wang, "Investigating haze-relevant features in a learning framework for image dehazing," in *Proc. IEEE Conf. Comput. Vis. Pattern*

[11] Q. Zhu, J. Mai, and L. Shao, "Single image dehazing using color attenuation prior," in *Proc. Brit. Mach. Vis. Conf. (BMVC)*, Nottingham, U.K., 2014, pp. 1–10.

[12] Qingsong Zhu, Jiaming Mai, and Ling Shao, "A Fast Single Image Haze Removal Algorithm Using Color Attenuation Prior" *IEEE transactions on image processing*, vol. 24, no. 11, November 2015, pp 3522-3533.